Geodinamica Acta

ISSN: 0985-3111 (Print) (Online) Journal homepage: http://www.tandfonline.com/loi/tgda20

Looking inside Late Variscan tectonics: structural and metamorphic heterogeneity of the Eastern Southalpine Basement (NE Italy)

Luca Benciolini , M. Eliana Poli , Dario Visonà & Adriano Zanferrari

To cite this article: Luca Benciolini , M. Eliana Poli , Dario Visonà & Adriano Zanferrari (2006) Looking inside Late Variscan tectonics: structural and metamorphic heterogeneity of the Eastern Southalpine Basement (NE Italy), Geodinamica Acta, 19:1, 17-32, DOI: 10.3166/ga.19.17-32

To link to this article: http://dx.doi.org/10.3166/ga.19.17-32

Published online: 13 Apr 2012.

Geodinamica Acta

Geodinamica Acta 19/1 (2006) 17-32

Looking inside Late Variscan tectonics: structural and metamorphic heterogeneity of the Eastern Southalpine Basement (NE Italy).

Luca Benciolini [a*], M. Eliana Poli [a], Dario Visonà [b], Adriano Zanferrari [a]

[a] *Dipartimento di Georisors e Territorio, Università di Udine, Via Cotonificio 114, I-33100 Udine, Italy*
[b] *Dipartimento di Mineralogia e Petrologia, Università di Padova, Corso Garibaldi 37, I-35137 Padova, Italy*

Received: 05/07/05, accepted: 23/01/06

Abstract

The Eastern Southalpine Basement on the southern side of the Brixen granodiorite pluton is comprised of two rock volumes separated by a shear zone and characterised by contrasting thermo-mechanical evolutions. The first rock volume appears in three different areas within hectometric folds consisting of amphibolite-facies paragneiss with polyphase structural and metamorphic evolution: a) D1 developed in HT-MP conditions: the assemblage Qtz + Pl + Bt + Kfs + Grt assemblage is preserved within D1 microlithons ; b) D2 is recorded in HT-LP conditions. Assemblages Bt + And + Crd, and Qtz + Kfs + Sil + Pl + Crn, developed within the differentiated S2 layering ; c) D3 developed in greenschist-facies, characterized by assemblage Ser + Qtz + Chl + Ab ; d) the contact aureole of the Brixen granodiorite pluton generating static growth of biotite, andalusite II and cordierite II at 282 ±14 Ma.
The second rock volume corresponds to the Brixen – Sarntal metamorphic basement described in the literature, and consists of greenschist-facies metapelite.
Field relationships indicate that HT-LP metamorphism took place before emplacement of the Brixen granodiorite and that paragneiss and metapelite were probably coupled at 320Ma, whereas the metamorphic aureole statically overprints the dynamic events and seals the contact.

Keywords : Eastern Southern Alps/Variscan orogeny/orogenic collapse

1. Introduction

Until the end of the 1980s, the Southalpine Basement was regarded as a structurally homogeneous sector of the South European Variscan Belt, in which regional metamorphism is of progressively lower grade from a granulite zone in the west (Ivrea – Verbano Zone) to an anchi-metamorphic zone in the east (western Paleocarnian Chain [1, 2]).

After the pioneering works of Brodie and Rutter, Handy, and Schmid *et al.* [3-5], several recent papers have pointed out the complexity of the Southalpine Basement. The presence of structural units characterised by contrasting pre-Alpine thermo-baric evolution has been documented in the western and central sectors of the Southern Alps [6-11] and the importance of a Permo-Triassic extension-related event has been recognised [3-6, 12-19].

The aim of this paper is to present structural and petrographical data on the polyphase evolution in metapelites from two key areas in the Eastern Southalpine Basement (Figs. 1, 2): i) the Middle Eisacktal/Media Val d'Isarco, near Brixen/Bressanone ; ii) the Sulzspitz/Cima Sulz area in Sarntal/Val Sarentino.

In order to place these results in the regional tectonic context, a review of existing data on the Eastern Southalpine Basement is proposed in section 6.2. The resulting tectonic evolution of the Eastern Southalpine Basement is depicted in section 6.3.

* Corresponding author.
Tel/Fax: +39 0432 558720 - *Fax:* +39 0432 55870
E-mail address: luca.benciolini@uniud.it

Table 1

	AGORDO		SARNTAL				BRIXEN (a)			BRIXEN (b)			PUSTERTAL		
	D1	D2	D1	D2	D2 ML	D3	D1	D2	D3	D1	D2	D3	D1	D2	D3
Quartz	—	—	—	—		—	—	—	—	—	—	—	—	—	—
Albite	—	—	—	—		—	—			—	—	—	—	—	—
Muscovite	—	—	—	—		—	—			—	—	—	—	—	—
Chlorite	—	—	—	—		—		—	—	—	—	—	—	—	—
Epidote	—		—	—						—	—				
Almandine	----			—			—	—	—		—				
Opaques	—	—	—	—			—			—	—				
Biotite	—			—				—	—		—				
K-feldspar								—	—						
Oligoclase					—			—	—						
Hornblende					—										
Chloritoid	----			—							—				
P (Gpa)			0.4		0.4	0.4	0.45-0.6	0.5-0.65	0.2-0.45	0,3	0.3-0.4		400-500	400-500	300-400
Method (P)					1	2	3	4	4	6	6		5	5	5
T (° C)					520		< 420	450-550	420-520	400	500-540	400			350-400
Method (T)					1		2	5	2	2	2				2
°C/Km					39			21-33		40	38-54				26-40
age (Ma)						325									316

Table 1

Tectonometamorphic evolution of Eastern Southalpine Basement. Data source: Agordo: [31]; Sarntal: [29]; Brixen (a): [28]; Brixen (b): [30]; Pustertal: [27]. D1, D2, D3 refer to GFM units, D2ML to interbedded Metabasic Layers [29]. T and P methods as follows: 1) Hornblende – oligoclase equilibria, [65]; 2) qualitative evaluation (T based on quartz plasticity and biotite isograd); 3) Plagioclase – biotite – garnet – muscovite barometer [66]; 4) Phengite barometer [67]; 5) Biotite – garnet equilibria [68, 69]; 6) Muscovite b_0 value [70].

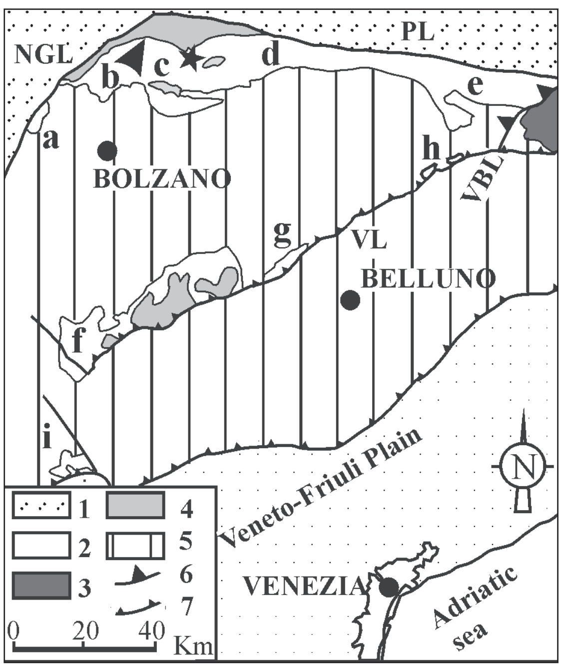

Fig. 1 – Sketch map of Eastern Southalpine Basement.

1) Austroalpine domain; 2) Metamorphic basement of Southern Alps; 3) Paleocarnian Chain; 4) Upper Paleozoic plutons; 5) Permo/Cenozoic cover; 6) Variscan thrust; 7) Valsugana (VL) thrust and present day front of eastern Southern Alps..

a = Ultental; b = Sarntal Alps; c = Brixen; d = Pustertal; e = Carnian Alps; f = Valsugana; g = Agordo; h = Comelico; i = Recoaro.

Star: Middle Eisacktal; arrow: Sulzspitz. NGL = North Giudicarie Line; PL = Pusteria Line; VBL = Val Bordaglia Line; VL = Valsugana Line.

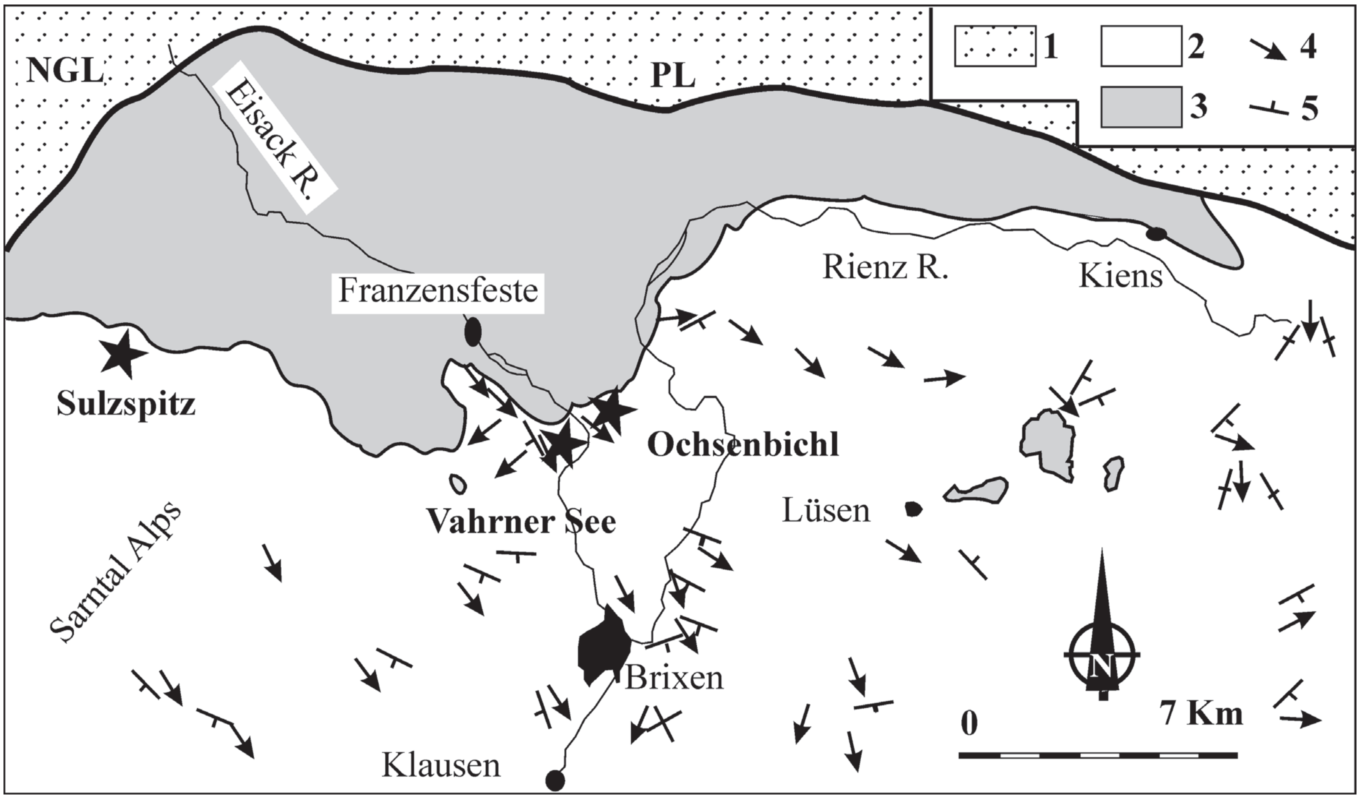

Fig. 2 - Structural map of westermost portion of the Eastern Southalpine Basement and Brixen pluton.

NGL = North Giudicarie line; PL = Pusteria line. Stars: study areas.

1) Austroalpine domain; 2) Southern Alps; 3) Permian intrusive bodies; 4) B3 fold axis; 5) S3 foliation.

2. Geological setting of Eastern Southalpine Basement

The Eastern Southalpine Basement represents a portion of the European Variscan Belt, and is bounded along its northern and western edges by two branches of the Periadriatic Lineament, i.e., the Pustertal/Val Pusteria and North Giudicarie faults (Fig. 1). To the east, the Val Bordaglia Line separates the Variscan basement from the anchi- to non-metamorphic Paleocarnian Chain [20-23] Basement rocks within the Eastern Southern Alps are limited to a few outcropping areas scattered over a region of some thousands of km^2 (Fig. 1). Petrological and structural research on this basement has traditionally focused on the areas of Agordo (g in figure 1), Pustertal (d in figure 1) and Sarntal/Val Sarentino (b in figure 1) with Brixen/Bressanone (c in figure 1) which is the westernmost portion of the Eastern Southalpine Basement. In the Sarntal-Brixen Metamorphic Basement, metapelitic and metapsammitic sequences of greenschist-facies prevail and have been attributed to the Early Palaeozoic [24]. Interbedded felsic (Comelico Porphyroids, Lower Ordovician [25]) and mafic (Gudon Fm., Early Silurian [26]) metavolcanic layers are also described in this area.

Structural studies in the entire Eastern Southalpine Basement have revealed three generations (D1, D2, D3) of syn-metamorphic structures (folds and foliations) which may be distinguished on the basis of overprinting criteria [20, 22, 27, 28].

Mineral assemblages syn-kinematic with events D1, D2 and D3 in various parts of the Eastern Southalpine Basement are listed in Table 1. Only the last group of structures (D3) is marked by the same mineral paragenesis, whereas mineral assemblages D1 and D2 show differences covering the whole greenschist-facies [27-31]. Radiometric determinations for the Eastern Southalpine Basement place the metamorphic thermal peak at about 350 Ma [32, 33]. White mica K-Ar and Ar-Ar cooling ages indicate cooling below 350°±50° C at 325±2 Ma (Sarntal) [34] and 316±8 Ma (Pustertal) [32]. These ages may reasonably attributed to event D3, which developed under T = 350-400°C [27].

The southern border of the pluton is characterised by scattered outcrops of metapelite affected by contact-metamorphosis, limited to sparse crystallisation of reddish-brown biotite and rare andalusite crystals [38, 40, 41]. Contact metamorphism is described as responsible for static crystallisation up to 200 m from the granodiorite border [40]. However Scolari and Zirpoli [41] noted that, at Ochsenbichl, Vahrner See and Alpe di Tramin (Sulzspitz), within banded gneiss of presumed migmatitic origin static biotite and andalusite are accompanied by cordierite.

3. Structures of HT metapelites and emplacement of Brixen Granodiorite

The Brixen granodiorite crosscuts all the regional structures (D1, D2, D3) of the surrounding basement. Neither magmatic flow structures nor shear zones related to the emplacement of the pluton have been observed. Figure 2 shows new data on the

D3 structural trend in the whole Sarntal-Brixen metamorphic basement. The data show that folds preserve the same style and orientation over a wide area and appear to be unaffected by the emplacement of the granodiorite.

Scolari and Zirpoli [41] interpreted the cordierite-bearing metapelite around the Brixen granodiorite as the product of contact metamorphism. Nevertheless it is scattered around a pluton responsible for the development of low-grade contact metamorphism [40].

Instead our work on these areas revealed that the biotite, cordierite and andalusite assemblage statically overgrows earlier foliations, as indicated by amphibolite-facies metamorphic minerals (Fig. 3). In order to determine the nature of these foliations, and their relations with the Brixen granodiorite and the surrounding greenschist-facies basement rocks, the three areas are described separately although, as shown in tables 2 and 3 and figure 4, they have very strongly similar features. At Ochsenbichl, Vahrner See and Sulzspitz, the foliations display the same syn-kynematic mineral assemblages. Deformations in these areas are hereafter considered as a single sequence of events and are labelled "p" (paragneiss): $D1_p$, $D2_p$, DM_p, and $D3_p$, whereas D1, D2 and D3 are referred to the Greenschist-Facies Metapelite of the Sarntal-Brixen metamorphic basement (hereafter GFM). Accordingly, the Middle Eisacktal and Sulzspitz Amphibolite-Facies Paragneiss (hereafter AFP) are considered a single geological unit.

	D1p	D2p	D3p	DMp	GD
Sulzspitz (SA)		—	—	—	—
Vahrner See (ME)	—	—	—	—	
Ochsenbichl (ME)	—	—	—		—

Table 2 : Paragneiss features at Sulzspitz, Sarntal Alps (SA) and Middle Eisacktal (ME) ; GD: Granodiorite Contact.

3.1. Sulzspitz area

Field observations collected in the Sulzspitz area are shown in figure 4b and 4c. The area is characterised by a hm-scale unroofed $D3_p$ fold with an axis trending towards N115° of 35° (Figs. 4c, 4d).

The inner side of the Sulzspitz fold contains lenses of garnet-bearing amphibolite-facies paragneiss (AFP, Fig. 5a ; cfr. 2 in figure 4b), whereas the surrounding Eastern Southalpine Basement is characterised by the metapelite and metapsammite of the GFM [27, 28, 42, 43] (cfr. 1 in figure 4b). The AFP structure is dominated by a penetrative $D2_p$ foliation

Fig. 3 - Contact metamorphism in study area, represented by mm- to cm-sized andalusite (And), cordierite (Crd) and biotite (Bt) crystals sealing Variscan-age sillimanite-bearing foliations (S2p). Scale bar: 0.5mm. a): Ochsenbichl; b) Vahrner See; c) Sulzspitz d): Ochsenbichl, euhedral undeformed andalusite grains (arrows) sealing F3p folds (dashed lines).

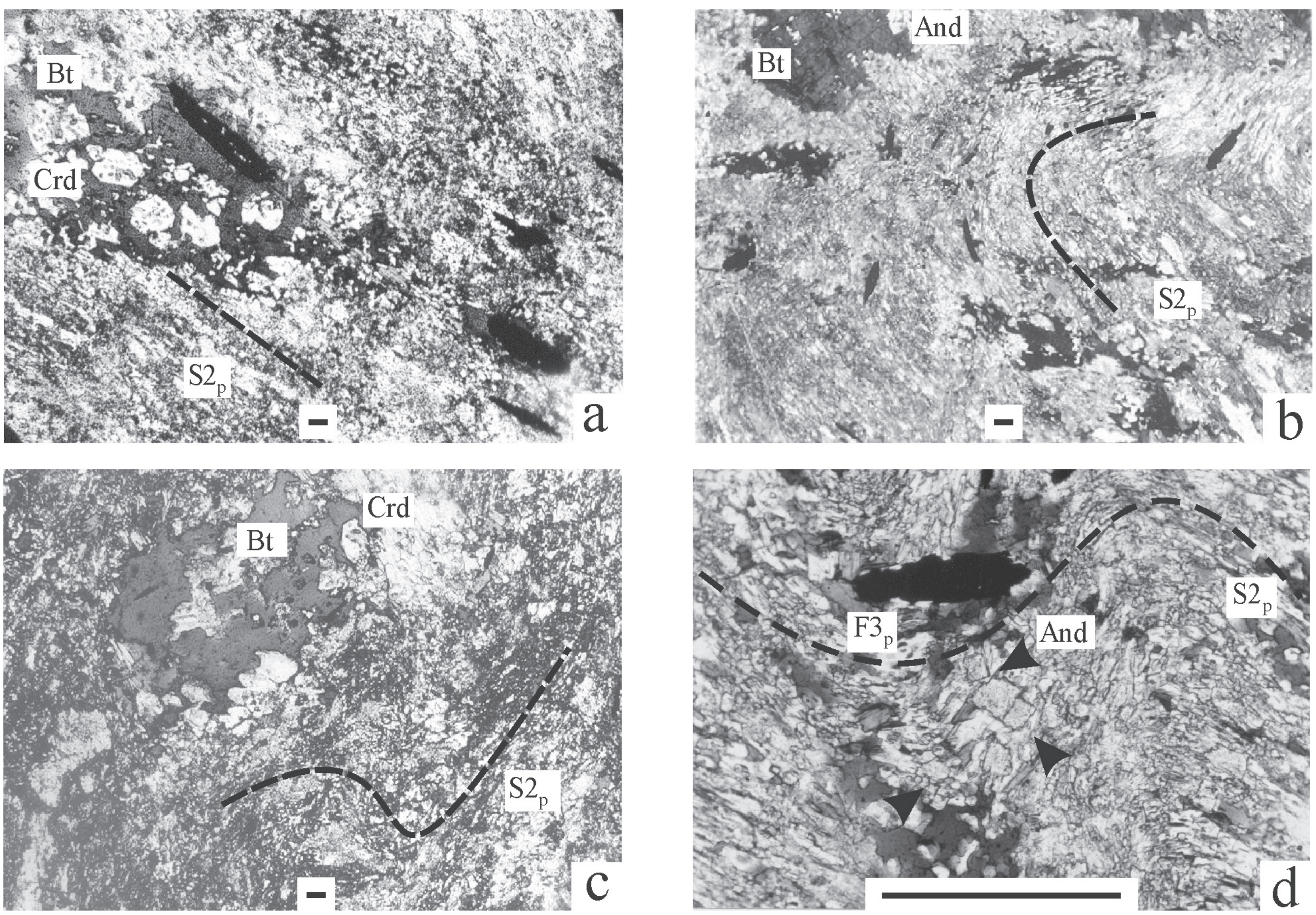

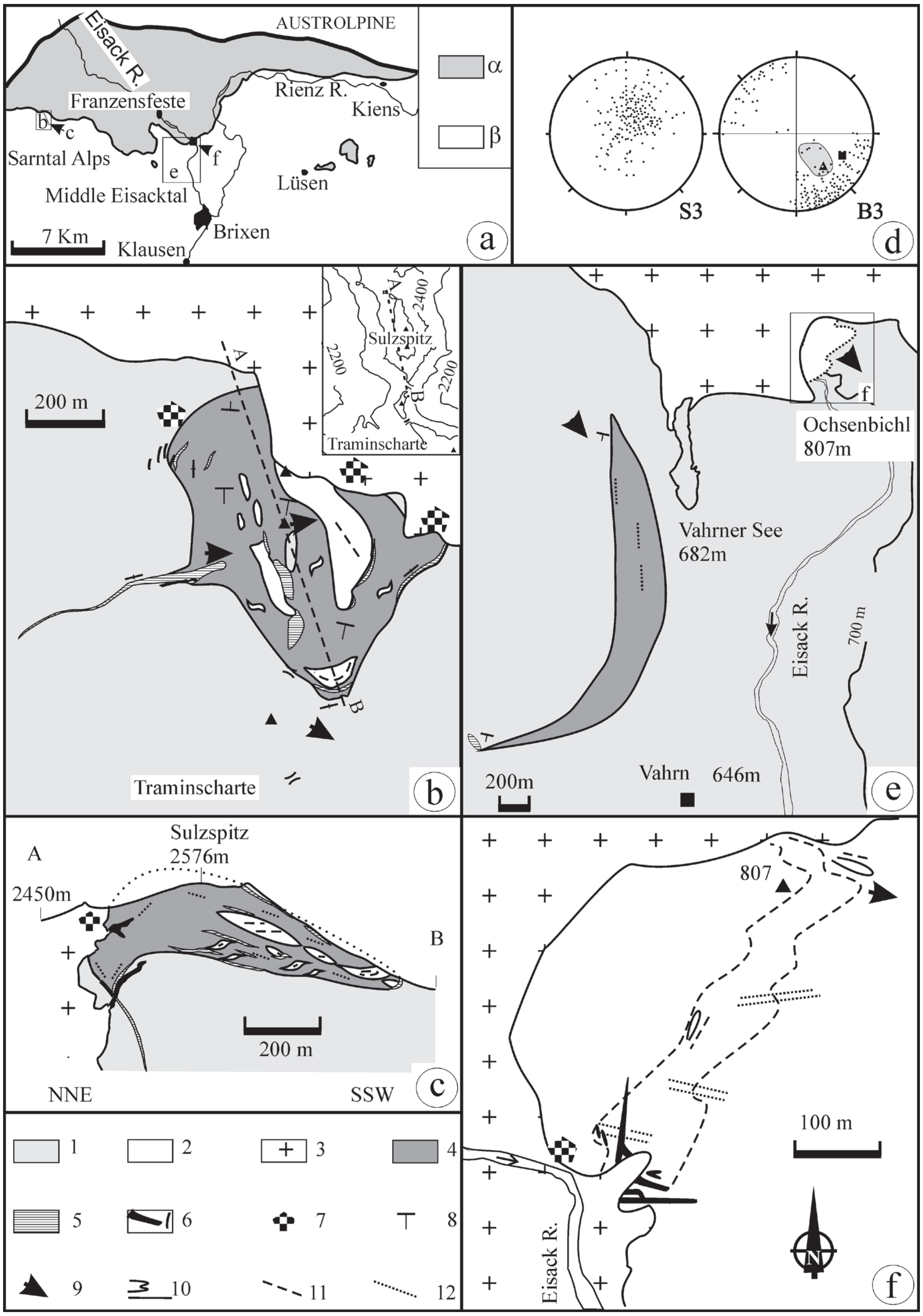

Fig. 4 - Geology of study areas.

a) Index map of study areas (inserts and arrows; cfr. Figure 2). Bold line: Periadriatic Lineament; α: Permian Intrusives; β: metamorphic basement.

b) Geologic sketch of Sulzspitz area, Sarntal Alps. A-B dashed line: location of cross section c;

c) Cross-section of the Sulzspitz area (b box).

d) Plot of S3 foliations and B3 mesofolds (Schmidt diagram). Shaded area: Ochsenbichl (f box); Triangle: Vahrner See (e box); Square: Sulzspitz (b box)

e) Geologic sketch of Middle Eisacktal area. Insert: location of box f;

f) Structural sketch of Ochsenbichl area.

LEGEND FOR THE GEOLOGIC SKETCH AND CROSS SECTION
1): Greenschist-facies metapelite and metapsammite of GFM unit;
2): AFP unit (this work);
3): Brixen granodiorite;
4) shear zone;
5) fine-grained quartz-rich mylonite;
6) granite dykes;
7) magmatic breccia;
8) mylonitic foliation;
9) D3 fold axes and stretching lineation;
10) S1p structural trend;
11) S2p structural trend;
12) S3p structural trend.

progressively crenulated and sheared by mylonitic event DM_p. $D2_p$ is preserved within lenses corresponding to relatively low strained domains; a thick shear zone (DM_p) separates the AFP and GFM units (cfr. 4 in figure 4b). In the field, the shear zone grades from sheared AFP paragneiss to a tectonic mélange with the surrounding GFM. Where metapsammitic lithologies prevail in the basement, homogeneous, fine-grained, quartz-rich mylonite is observed (Fig. 5b; cfr. 5 in figure. 4b).

Quartz stretching lineations on both sides of the Sulzspitz fold trend towards N 80° to 100° by 15° to 50°. A cm-spaced axial plane foliation develops only close to the fold hinge. In the Sulzspitz area, the rock fabric progressively grades from the banded gneiss of the basement to the mylonite of the shear zone. Thus, the geological boundary between shear zone and AFP given in figure 4b roughly corresponds to the first appearance of garnet and sillimanite relics. The boundary

Minerals	D1p	D2p	DMp	D3p	CM
Albite			—	—	
Andalusite		—			—
Biotite	—	—			—
Chlorite			—	—	
Cordierite		—			—
Corundum		—			
Garnet	—				
K-Feldspar	—	—			
Muscovite			—	—	
Plagioclase	—	—			
Quartz	—	—	—	—	
Sillimanite	—	—			

Table 3 : occurrence of mineral phases in Ochsenbichl paragneiss during three deformation events and during contact metamorphism (CM).

between greenschist-facies metapsammite and the shear zone roughly correspond with the evidence of tectonic mélange of quartz-poor paragneiss and metapsammite. Heterogeneous strain distribution is mainly due to the quartz content of the sheared lithologies (Figs. 5b and 8b): the strain was highly concentrated within quartz-rich lithologies.

A second large, open coaxial fold refolds the Sulzspitz $D3_p$ fold, leading to passive reorientation of planar $D2_p$ and DM_p fabrics. Lastly, the whole structure is truncated by the Brixen granodiorite (Fig. 4b). Style, orientation and metamorphic paragenesis of the fold (see later) indicate possible correlations with the D3 regional deformation which developed at 320 Ma (Figs. 2, 4d; see discussion).

The magmatic contact is sinuous and characterised by magmatic breccia. The paragneiss of the AFP unit, GFM metapsammite and quartz-rich mylonite occur as fragments in the magmatic breccia (Fig. 5c). Close to the granodiorite border, the mylonite is locally affected by the static growth of several cm-sized feldspar crystals (Figs. 5d, 8d).

3.2 Middle Eisacktal area

From Klausen in the south to Franzensfeste in the north (Fig. 2) the Eisacktal is a Pleistocenic glacial trough at 500 to 800 m a.s.l. filled by thick Pleistocene deposits [44]. Basement

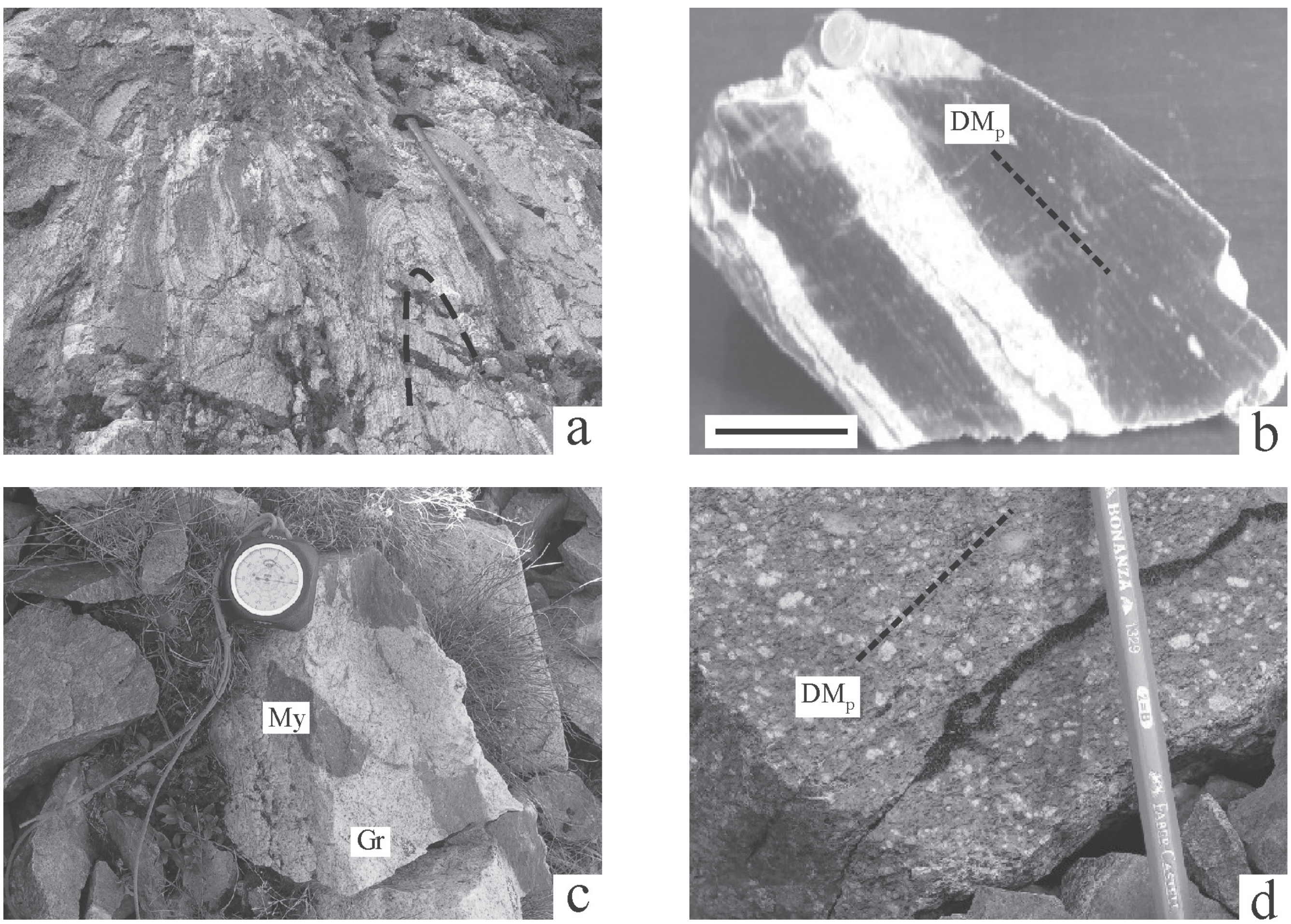

Fig. 5 - Field relationships at Sulzspitz
a): Garnet-bearing amphibolite-facies paragneiss (AFP unit) at hinge of hm-scale Sulzspitz fold; b) strain heterogeneity in Sulzspitz shear zone (DMp; see Fig. 10a; scale bar: 5cm): quartz-rich (black) high-strain levels alternate with albite-rich (white) low-strain domains; c) elements of Sulzspitz mylonite (My) in a magmatic breccia (Brixen granodiorite: Gr); d) cm-size K-feldspar blasts overgrowing the Sulzspitz mylonite (DMp) near Brixen granodiorite contact.

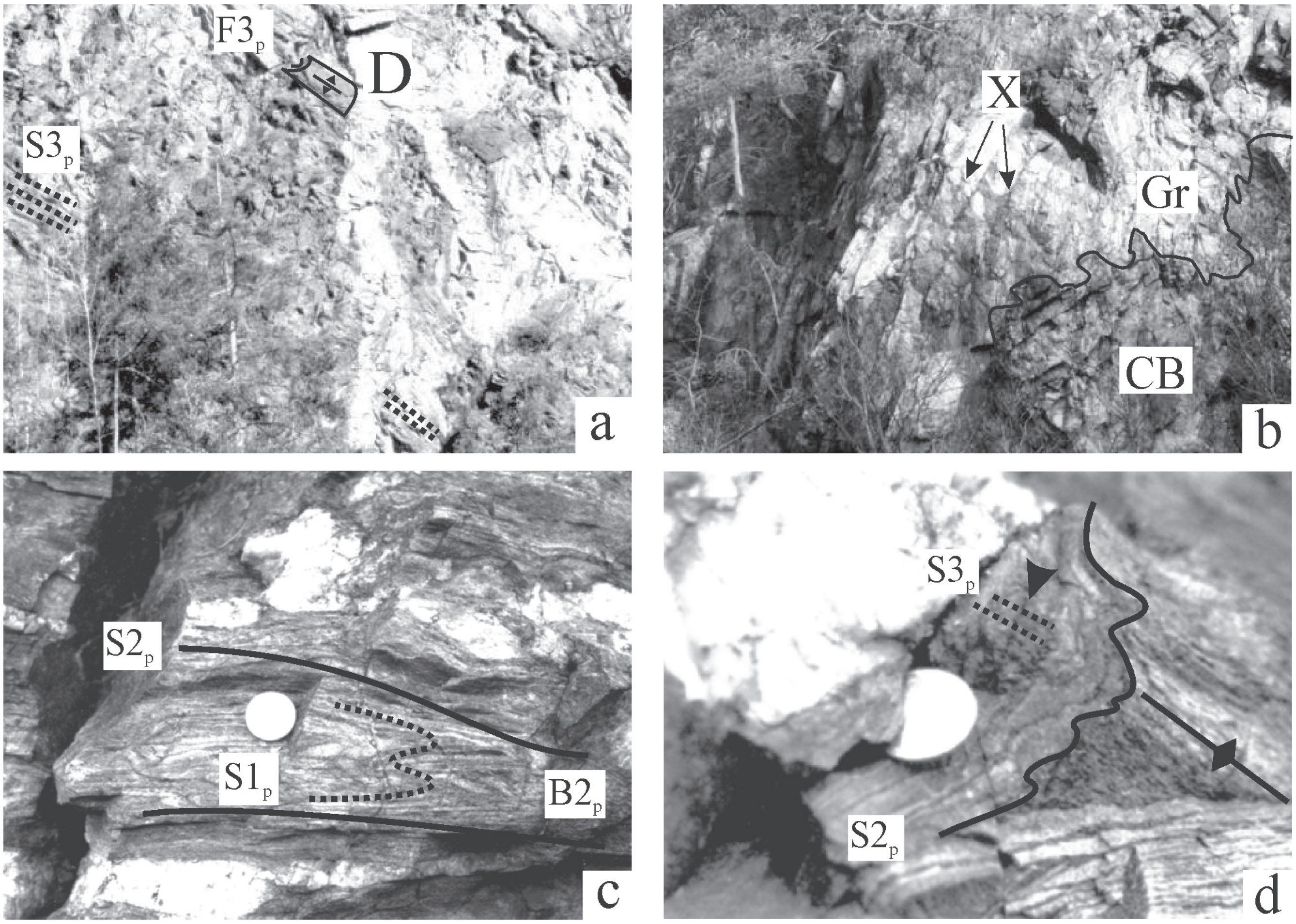

Fig. 6 – Field relationships at Ochsenbichl. a) granitic dyke (D) crosscutting S3p (dotted line) and F3p (arrow); b) metapelitic xenoliths (X, arrows) at granodiorite (Gr)/metapelite (CB) contact; c) S1p foliation and unroofed B2p relics locally preserved within a thicker felsic S2p layer; d) S3p crenulation cleavage (arrow) developing within mica-rich layers on axial plane of F3p fold.

rocks are seen only in a few sparse outcrops, including the Ochsenbichl and Vahrner See localities (Fig. 2), known for the And + Crd + Bt paragenesis which developed during contact metamorphism (Fig. 3 [41]). Because of the limited outcrops available, geological relationships of the amphibolite-facies rocks with the surrounding lithologies are largely interpreted in the light of the Sulzspitz results. In contrast, the "*roches moutonnées*" at Ochsenbichl allowed detailed structural analysis of the amphibolite-facies basement rocks.

3.2.1 Vahrner See

Field observations in the area are shown in figure 4e.

The sparse outcrops show widely retrogressed AFP, suggesting many similarities with the sheared limbs of the Sulzspitz fold. Quartz-rich mylonite and a $D3_p$ hinge trending towards N140° by 45° are also shown. In figure 4e, a hm-scale $D3_p$ fold is assumed (table 2).

3.2.2 Ochsenbichl

Ochsenbichl is an extensive area of *roches moutonnées* in Eisacktal, near Brixen (Figs. 2, 4e). The outcrop area only covers a few thousand m^2. Well-defined field relations of the AFP unit with the Brixen granodiorite are visible, but relations with the GFM unit are not available (table 2). The Ochsenbichl is the most favourable area for understanding the metamorphic evolution of the amphibolite-facies rocks (Fig. 4f).

The granodiorite/metapelite boundary strikes approximately NE-SW and dips steeply SE. The AFP are intruded by a network of sharp, cross-cutting granitic dykes (Fig. 6a), which probably formed as a result of (brittle) host rocks fracturing. Once again, at Ochsenbichl the granodiorite/AFP boundary shows sinuous contacts and magmatic stoping structures (Figs. 4f, 6b), and clearly cuts any regional ductile structure (Figs. 4f, 6a).

The AFP are banded gneiss with cm- to dm- scale felsic layers alternating with dark biotite-rich layers. As reported by Scolari and Zirpoli [41], up to 5 mm–sized biotite flakes and millimetric andalusite blasts crosscut both dark and light layers. The most penetrative structure is a 20°-30° E- or SE-dipping foliation ($S2_p$), often characterised by well-developed gneissic layering with alternating quartz-rich and pelitic-rich layers. Relic $S1_p$ foliation and rootless $B2_p$ hinges are locally observed within $S2_p$, where the felsic layers are thicker (Fig. 6c).

$B3_p$ are tight 30° folds dipping towards SE, occasionally associated with penetrative cm-spaced $S3_p$ axial plane folia-

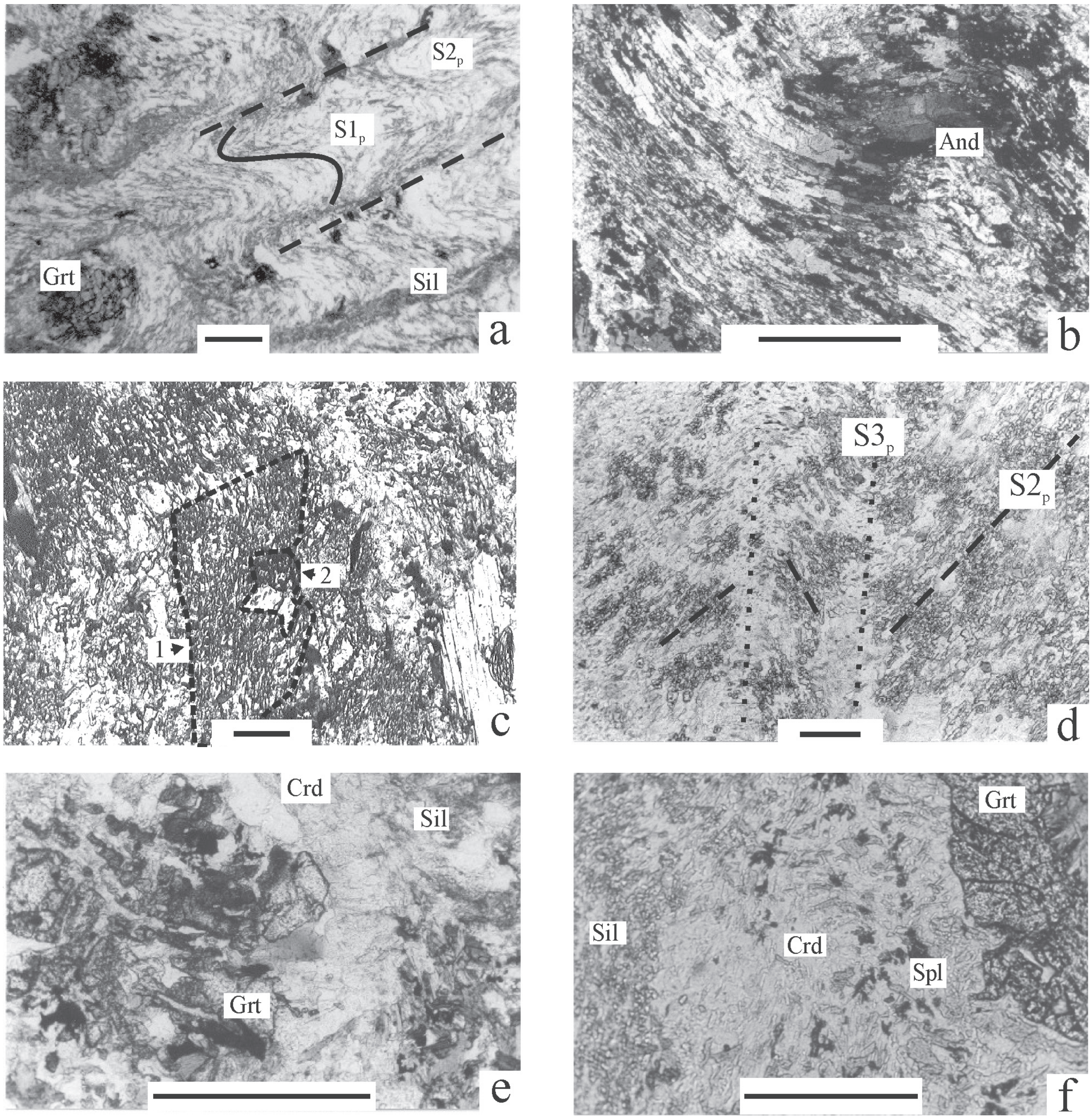

Fig. 7 –Petrographic and microstructural features of AFP unit. Scale bar:0.5mm. a) D1p garnet (Grt) -bearing relics within S2p sillimanite (Sil) bearing crenulation cleavage; b) dynamic recrystallisation of andalusite on S2p; c) Kfs + Sil assemblage (1) and Crn + Sil assemblage (2) replacing former muscovite; d) Sil + Kfs + Bt mineral assemblages growing on S2p foliation (dashed lines) are folded and replaced by chlorite + sericite + albite on S3p (dotted lines); e) cordierite (Crd) *corona* at garnet (Grt) contact with sillimanite - K-feldspar domain; f) cordierite and spinel (Spl) *corona* at garnet (Grt) contact with sillimanite (Sil) - K-feldspar domain.

tion (Fig. 6d), often developing only within mica-rich layers. $D3_p$ structures have the same style and orientation as those of the entire Eastern Southalpine Basement (Fig. 2). Locally, where $S3_p$ is particularly well-developed, gneissic layering is observed, with alternating quartz-rich, mica-rich and green chlorite-rich layers. $D3_p$ is the latest ductile structure.

The areal distribution of the $D3_p$ S and Z asymmetries indicates that as at Vahrner See and Sulzspitz, the AFP unit at Ochsenbichl may also appear in the core of a D3 hm-scale regional fold (Fig. 4f).

4. Microstructural and petrographic observations on amphibolite-facies metapelite

The microscopic features reported here are mainly observed on samples from Ochsenbichl (see figure 4f), where polished outcrops allow detailed mesostructural analysis and complete S1, S2 and S3 structural collection. Nevertheless, these observations also describe the Vahrner See and Sulzspitz AFP well. Instead, DMp samples are available only at Sulzpitz.

The metamorphic assemblages corresponding to the observed structural evolution ($D1_p$, $D2_p$, DM_p, $D3_p$) and to contact metamorphism are summarised in Table 3.

4.1. $S1_p$ foliation

$S1_p$, representing the earliest set of syn-metamorphic foliations, is a folded schistosity in $S2_p$ microlithons ; it is defined by the assemblage Qtz + Bt + Pl + Kfs + Grt (Figs. 6c, 7a).

4.2. $S2_p$ foliation

$S2_p$, is a pervasive schistosity representing the main regional foliation sometimes truncating $D1_p$ folds (Fig. 6c) or, on a microscopic scale, appearing as a crenulation cleavage (Fig. 7a). As usual, metapelitic rocks display the effect of strain partitioning [45] leading to differentiated mica-rich films (M domains) alternating with quartz- and feldspars-rich layers (Q domains), characterised by relatively more competent mineral phases.

Within the $S2_p$, M and Q domains have contrasting chemical compositions, metamorphic parageneses and microstructures. Bt + And + Crd occupy the M domains, and occur as deformed crystals with dynamically recrystallised rims (Fig. 7b).

The Q domains contain ribbons of K-feldspar and microlitic sillimanite alternating with ribbons of quartz + plagioclase + K-feldspar. Clusters of K-feldspar and corundum are also occasionally observed within the Q domains (Fig. 7c).

Quartz, plagioclase and K-feldspar clearly show rational grain boundaries, suggesting equilibrium. Sillimanite mainly appears within these relatively less deformed domains, in submillimetric inclusions within K-feldspar. K-feldspar and sillimanite are in turn restricted to two-mineral layers. Because of its morphology, sillimanite escaped the strain concentration commonly observed in fibrous sillimanite [46]. Garnet relics and reactional textures are often observed within Q-domains. Cordierite *coronae* (Fig. 7e) and rare cordierite + spinel coronae (Fig. 7f) are developed around garnet at the contact with the K-feldspar-sillimanite layers.

4.3. $S3_p$ foliation and greenschist-facies events

$S3_p$ appears as a cm-spaced crenulation cleavage (Fig. 6d), emphasized by a Ser + Qtz + Chl + Ab assemblage (Fig.7d), obliterating the earlier high-temperature mineral assemblages. Relics of $S2_p$ mineral phases, such as biotite-rich films, relict garnet and corundum, andalusite and sillimanite, rimmed or replaced by sericite, are frequently observed on a millimetric scale.

The same mineral paragenesis is also observed within the shear zone described at Sulzspitz. Here, both AFP and GFM lithologies contribute to generate mylonite (Fig. 8a). In the mylonitic fabric, relatively undeformed feldspar-rich domains alternate with quartz-rich mylonite characterised by a 0.1mm grain-size and a Qtz + Chl ± Ab assemblage ; Figs. 5b and 8a). The AFP $D2_p$ fabric may be sharply truncated by fine-grained quartz-rich mylonite, but more commonly the GFM planar fabric and related mineral assemblage is gradually substituted. In this case, within the metapelite progressive chloritisation of garnet, biotite and cordierite and transformation of feldspars, andalusite and sillimanite to muscovite and albite accompany grain size reduction. The same mineral assemblage is observed in the axial plane foliation of the Sulzspitz $D3_p$ fold.

4.4. Contact metamorphism

Low-pressure static recrystallisation of andalusite II is represented by submillimetric grains replacing sillimanite and by scattered millimetric to centimetric euhedral grains. The latter overgrows both dark mica-rich and light felsic layers. Some scattered euhedral cordierite crystals and red biotite flakes also show a post-kinematic character. This recrystallisation is weakly dependent on distance from the pluton, clearly follows $D3_p$, and never masks any previous regional structure (Fig. 3d). Close to the granodiorite contact, mylonite may be included within magmatic breccia (Fig. 5c). This process is accompanied by an increase in the size of quartz and albite, whereas chlorite and muscovite generate new biotite grains organised in rounded polycrystalline aggregates (Fig. 8c). Some idiomorphic microcline crystals also overgrow the mylonite close to the granodiorite contact (Figs. 5d, 8d). They clearly confirm that granodiorite emplacement followed the tectonic coupling of the AFP and GFM units. Due to the absence of potassium within the host qtz- mylonite, the possible metasomatic origin of these feldspars is hypothesised.

4.5. Coronitic textures

In order to define the relative timing of the described reactional textures (Figs 7e, 7f) responsible for the development of static recrystallisation, we make the following observations:

- reactions around garnet producing Crd or Crd + Spl *coronae* respectively are observed only in samples recording $D2_p$. Both reactions are known to be pressure-sensitive ;
- if coronitic cordierite and spinel formed during contact metamorphism, they should be accompanied by K-feldspar, implying temperatures as high as 650° C [47].

Thus, the absence of K-feldspar and the accompanying aureole parageneses (see sections 4.4 and 5.5) indicate that the two *coronae* formed between $D1_p$ and $D2_p$. Strain partitioning during $D2_p$ allowed these textures to be preserved.

5. Qualitative thermal evolution of the AFP unit

As described above, events $D1_p$ and $D2_p$ record similar assemblages, since they include biotite, sillimanite and K-feldspar. $D2_p$ also shares biotite, cordierite and andalusite

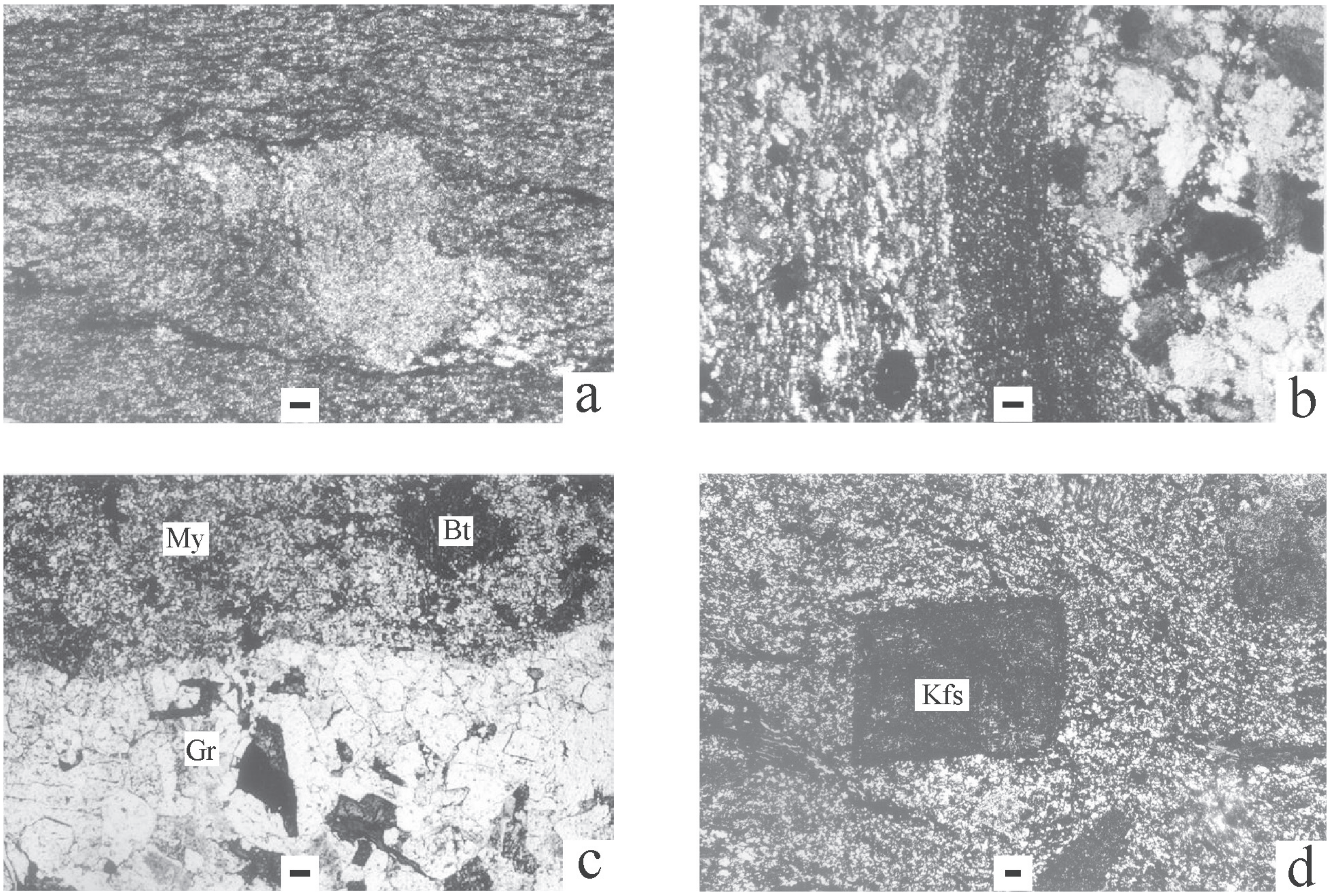

Fig. 8 – Microstructural features of Sulzspitz mylonite. Scale bar: 1mm. a) K-feldspar clast within a fine-grained quartz-rich matrix; b) Strain heterogeneity within Sulzspitz shear zone (see Fig. 5b). Different quartz content in protolith (higher in middle, lower on right) explains behaviour of sheared GFM lithologies; c) Recrystallisation of a mylonitic xenolith within a magmatic breccia (see figure 5c). Gr: granodiorite; My: mylonite; Bt: biotite aggregate; d) K-feldspar blasts overgrowing Sulzspitz mylonite (see figure 5d).

with contact metamorphism. However, there are systematic differences in the mineral assemblages of samples collected from different structures (table 3). For example, sample fabrics recording $D1_p$ never contain andalusite or cordierite; sample fabrics recording $D2_p$ never reveal equilibrium contacts of garnet with Al_2SiO_5, and contact metamorphism never involves sillimanite. We suggest that $D1_p$ and $D2_p$ represent distinct stages of mineral crystallization, and argue that the AFP unit underwent decompression between $D1_p$ to $D2_p$, before the $D3_p$ retrogression stage.

The parageneses presented above are discussed in the petrogenetic grid for the K_2O-FeO-Al_2O_3-SiO_2-H_2O system proposed by Xu *et al*. [47]. Our qualitative estimates are based on 63 samples collected from an wide outcrop of 15,000 m^2 (Fig. 4f). In our opinion, they clearly encompass the overall structural and microstructural evolution observed in this area and thus successfully describe the evolution of the AFP as a whole.

$D1_p$ relics are limited to the felsic domains. The mineral assemblage comprises Grt + Sil + Bt + Kfs + Pl. The paragenesis is limited by reaction Grt + Sil = Crd + Spl towards low pressure, reaction Ms + Qtz = Kfs + Sil towards low temperature, and reaction Bt + Sil = Kfs + Spl + Grt towards high temperature.

The $D2_p$ mineral assemblage includes Qtz + Bt + And + Sil + Kfs + Crd + Pl. In a few $D2_p$ samples, spinel and corundum occur sparsely.

In low-pressure metapelite, the corundum + K-feldspar assemblage (Fig. 7c) appears as the result of the muscovite breakdown reaction: Ms = Crn + Kfs. Muscovite is completely absent before $D3_p$ and probably disappeared at a lower temperature through the reaction Ms + Qtz = Kfs + Sil. Thus, the rare corundum crystals, observed within relatively less deformed Q domains, may derive from the breakdown of rare muscovite relics (Fig. 7c). In the studied paragneiss, spinel only occurs in rare spinel + cordierite *coronae* around garnet (reaction Grt + Sil = Crd + Spl). Spinel growth is not favoured because, during thepressure decrease after D1p, sillimanite-garnet contacts were already armoured by cordierite (reaction Grt + Sil+ Qtz = Crd). During the following evolution, reaction Bt + Ms+ Sil = Kfs + Spl was not favoured by the lack of muscovite, like reaction Bt + Sil = Crd + Spl + Kfs because biotite and sillimanite were confined to different microstructural domains, and reaction Bt + And = Crd + Spl + Kfs may have recovered during the long post-D2 thermal history. Lastly, we argue that the $D2_p$ assemblage is limited by the following reactions: 1) Sil = And; 2) Ms = Crn + Kfs and 3) Bt + Crd = Kfs + Grt + Spl.

In summary, amphibolite-facies metamorphic evolution (D1p to D2p) is consistent with T ≥ 600-650°C during a decompression path from unknown higher pressure to about 0.2-0.3 GPa.

Retrogression followed, with Ser + Qtz + Chl + Ab during $D3_p$. This mineral assemblage is common throughout the Eastern Southalpine Basement and corresponds to coeval structures (Fig. 2, Table 1). Accordingly, we suggest metamorphic conditions of T = 350°-400° C and P = 0.2–0.4 GPa during D3 [27, 47].

Lastly, intrusion of the Brixen granodiorite at 282 ±14 Ma generated static growth of reddish-brown biotite, andalusite and cordierite in the country rocks implying metamorphic conditions of T up to 629° C and P ≤ 0.26 Gpa [37, 47].

Figure 9 compares the thermal evolution of the AFP unit with the surrounding GFM unit.

6. Discussion

Detailed structural analysis of three key localities in the Eastern Southalpine Basement indicates the presence of two rock volumes with differing metamorphic and structural evolutions and therefore representing different tectonic units.

At Sulzspitz, Vahrner See and Ochsenbichl, rock volumes with HT-LP metamorphic parageneses (AFP) are separated from the surrounding greenschist-facies basement (GFM) by a thick shear zone (Fig. 4). This shear zone is older than the emplacement of the Brixen granodiorite (282 Ma), as clearly demonstrated by field relationships.

As regards the contact of the Brixen granodiorite with the country rocks, our data show that:

1) the granodiorite intrusion cuts all ductile structures observed in the Ochsenbichl area (Figs. 4, 5c, 6a);
2) static contact metamorphism seals $D3_p$ folds (Fig. 3d);
3) no magmatic flow structures are observed or described in the literature on the Brixen granodiorite;
4) the contact between granodiorite and country rocks is characterised by a network of sharp, cross-cutting granitic dykes and magmatic breccia (Figs. 4, 6a, 6b);
5) structures in the host rocks are unperturbed by the granodiorite intrusion (Fig. 2).

These observations confirm that the Brixen granodiorite is a «discordant pluton» which ascended permissively within a cold brittle crust [48, 49].

This conclusion fits previous works on some of the Variscan plutons in the Central and Eastern Southern Alps [37, 39, 50, and references therein] and indicates that, in these cases, all the foliations observed in the basement must be referred to Variscan regional events.

The Ochsenbichl, Vahrner See and Sulzspitz (Alpe Tramin) are known in the literature because of their peculiar paragenesis of contact metamorphism, characterised by cordierite, andalusite and biotite, never observed elsewhere. In order to explain this peculiar paragenesis, we infer that here, unlike the surrounding GFM unit, andalusite and cordierite crystallisation was favoured energically by their former presence within the $D2_p$ regional foliation. As regards the hypothesis of Scolari and Zirpoli [41], we stress that no migmatite is observed in the area and that the banded gneiss clearly shows structures and mineral assemblages unrelated to granodiorite emplacement.

As expected near granodioritic plutons emplaced at shallow depths within high-grade rocks [51], contact metamorphism only appears within a narrow aureole where sparse minerals grow or recrystallise under static conditions, whereas older fabrics are always wholly preserved.

Relationships between the AFP and the surrounding GFM basement are fully consistent with the presence of hm-scale $D3_p$ regional folds. If the correlation of these folds with the D3 regional event is correct, the metamorphic evolution of the AFP is older than 320 Ma. Accordingly, in the following we describe the Variscan evolution of the Eastern Southalpine Basement.

6.1 AFP evolution

Amphibolite-facies rocks are here described the first time in the Eastern Southalpine Basement. These rocks show high temperature–low pressure paragenesis, which retrogressed both along a shear zone and during the D3 regional event.

6.1.1. HT-LP Variscan event

The data given above indicate that the metamorphic evolution of the AFP in the Eastern Southalpine Basement refers to a Variscan regional event. In figure 9, this thermal evolution is qualitatively compared with the PTt path reconstructed in the surrounding basement [27, 28]. According to radiometric regional estimates, the Variscan thermal peak is commonly attributed to the Late Devonian-Early/Middle Carboniferous (350 Ma [32, 33, 52, and references therein]. This time-span overlaps the exhumation history of the Ultental/Val d'Ultimo high-pressure rocks (360-300 Ma [53]). Bearing in mind these regional data, we suggest 350 Ma as the age of the thermal peak in the AFP.

6.1.2. Greenschist-facies retrogression

In the study area, the same greenschist-facies mineral assemblages with Qtz + Chl + Ms accompany both the coupling of the greenschist-facies basement and the amphibolite-facies rocks (DMp) and the D3 folds in the Eastern Southalpine Basement as a whole (Fig. 7d, Tables 1 and 3). According to literature data, this event developed in metamorphic conditions of T=350°-400° C and P = 0.2–0.4 GPa [27]. We suggest that both these events were effects of the same tectonic regime responsible for the Late Carboniferous exhumation of the Variscan basement. In the following, both the rock volumes underwent together the emplacement of the Brixen granodiorite and the Alpine orogenic cycle.

6.2. Eastern Southalpine Basement evolution : a critical assessment

At Ochsenbichl, the style and sequence of deformation are the same as those in the surrounding Eastern Southalpine

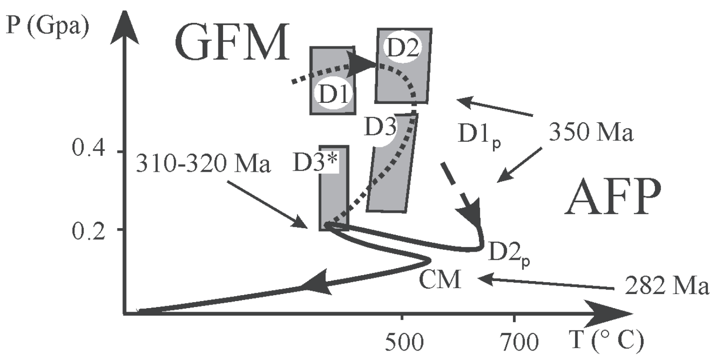

Fig. 9 – P-T-t path of greenschist-facies metapelite of Brixen area (GFM) and amphibolite-facies paragneiss of Ochsenbichl area (AFP). P-T conditions during D1, D2 and D3 in GFM after Ring and Richter [28]; D3* after Hammerschmidt and Stöckhert [27, see text]; P-T conditions during D1p, D2p and CM (= contact metamorphism) in AFP: this paper.

Basement, which may have contributed towards masking until now the unusual metamorphic mineral assemblages reported here.

In order to compare our results with data from previous works, in the following we critically re-examine existing data on the Eastern Southalpine Basement.

6.2.1 Review of existing data

As already noted, basement rocks within the Eastern Southern Alps are limited to a small number of outcropping area scattered over a region of some thousands of km^2 (Fig. 1).

Mineral assemblages crystallising during D1, D2 and D3 in various areas of the Eastern Southalpine Basement (outside the study area), are listed in Table 1. Everywhere they compound a penetrative main foliation and a later tight to isoclinal folds, which refolded the previous schistosity and gave rise to axial plane foliation, emphasised by mica-rich layers. Relics of a planar anisotropy is frequently observed in dm-scale rootless folds at Brixen, Sarntal and Pustertal, but has never been observed at Agordo.

The main foliation (called S2 at Brixen, Sarntal and Pustertal, and S1 at Agordo) is characterised by a similar greenschist-facies mineral assemblage which shows small but important differences from north to south and eastwards. Quartz, albite, chlorite, epidote, biotite, almandine and chloritoid are common in S2 at Brixen (north [28]). In the Agordo area (south), almandine and chloritoid are very rare [26, 31].

Lower temperatures are recorded in Pustertal (east), where S2 is characterised by Qtz + Ab + Ep + Chl mineral assemblage [27].

The highest temperatures are recorded in Sarntal (NW corner of Eastern Southalpine Basement), where some D2 metabasic layers are described [29] (see D2ML in Table 2).

Consistently, pressure and temperature conditions of T = 520°C, P= 0.4 GPa (Sarntal [29]); T = 450-550°C, P = 0.5 – 0.65 GPa, (Brixen [28]) and T = 300-350°C, P= 0.2 – 0.4 GPa (Pustertal [27]) have been suggested in these areas (Table 1).

By contrast, the most recent metamorphic foliations (S3 in GFM at Brixen, Sarntal and Pustertal, S2 at Agordo), have the same mineral assemblage, with Qtz + Ab + Ms + Chl throughout the Eastern Southalpine Basement as a whole [26, 27, 29, 30] and in the study areas. Pressure and temperature conditions of 350-400°C and 0.3 – 0.4 GPa have been estimated for the Pustertal sector, pertaining to the mineral assemblages which crystallised during D3.

In the Brixen area, Ring and Richter [28] suggest a different estimate for D3 (T = 420-520°C). This value was obtained by including in the D3 mineral paragenesis both garnet («*grt2 grew during D2 and remained stable during D3*» [28]) and biotite («*Biotite overgrows D2- and D3-structures indicating that metamorphism outlasted deformation*» ; [28]). We suggest here that P-T conditions must be estimated on the basis of the set of minerals which actually crystallised during the deformation event. Thus, our preferred estimate of D3 P-T conditions is that given in Hammerschmidt and Stöckhert [27] (D3*, Fig. 9) ; the estimate of Ring and Richter [28] (D3 in figure 9), discordant with respect to all other literature data, is interpreted as pertaining to an earlier event, unrelated to the S3 foliation. These observations, the scattered outcropping area, the heterogeneity in outcrop ratio, and in the structural and metamorphic features documented here, all indicate the critical value of correlation criteria in interpreting geological data.

6.2.2 Correlation criteria

The increase in metamorphic grade from the east (Comelico, chlorite zone) to the north-west (Sarntal, almandine zone) has been evidenced since the 1970s [2, 54, 56]. According to the literature data, a thermal gradient of 30° ± 10° C/km during D1 and D2 may be inferred on the basis of metamorphic parageneses from various areas of the northern part of the Eastern Southalpine Basement. More recently, these petrologic arguments have been used to correlate all structural D1+D2 events identified in the Eastern Southalpine Basement [27, 28, 42, 43, 56]. The lack of outcrops, the lack of radiometric data, the uncertainties in pressure and temperature estimates (Table 1) and the scarcity of detailed analytical work, at present hamper validation of the above hypothesis.

The latest event only (D3 in the GFM at Brixen, Sarntal and Pustertal, D2 at Agordo) displays the same style, orientation and metamorphic mineral assemblages, is extensively recorded and may have the same temporal significance. Instead, the unusual HT-LP mineral assemblages of D1 and D2 which differ from these of the surrounding basement, may have developed in another tectonic setting.

In the present work, events identified in various outcrops and areas are correlated not only according to their deformation style but also according to their structural trends and time-equivalent mineral assemblages [57-60].

6.3. Geodynamic significance of metamorphic and structural events

Figure 10 shows the suggested tectonic evolution of the Eastern Southalpine Basement.

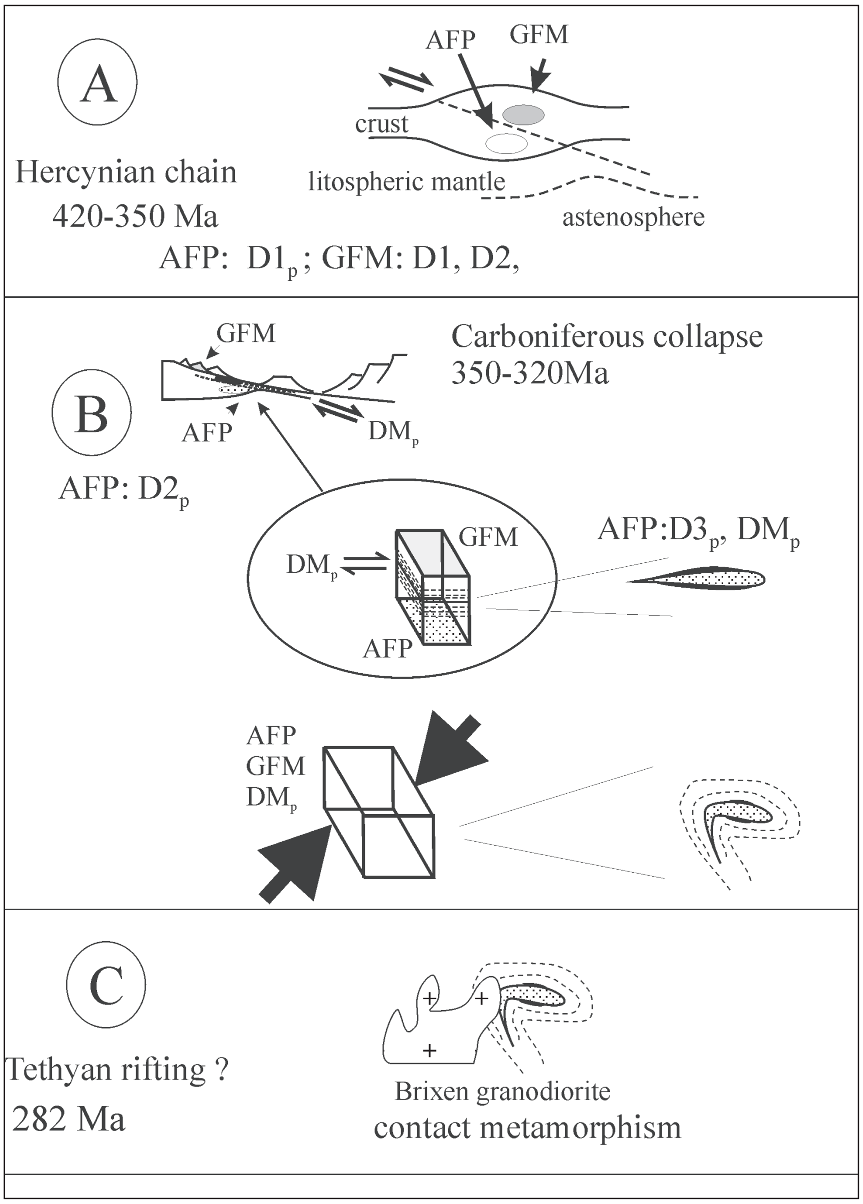

Fig. 10 - Tectonic cartoon showing evolution of Eastern Southalpine Basement.

Variscan thickened crust (A)

Eastern Southalpine Basement metapelite and metapsammite (GFM) underwent greenschist-facies metamorphism, D1 and D2 deformations, whilst AFP paragneiss underwent amphibolite-facies metamorphism during D1p deformation.

During following Carboniferous collapse (B)

- paragneiss (AFP) underwent amphibolite-facies metamorphism and $D2_p$ deformation;
- AFP and GFM were coupled along Sulzspitz Shear Zone (DMp);
- Eastern Southalpine Basement underwent D3 de formation; metapsammite was mylonitised.

During Permian magmatic events (C)

Eastern Southalpine Basement was intruded by granodioritic to dioritic plutons (e.g. the Brixen Granodiorite exhumed and covered by andesitic to rhyolitic flows of Athesian Volcanic District. The last event may correspond to early Tethyan rifting event.

In AFP $D1_p$ may be attributed to T ≥ 600° - 650°C and P > 0,3GPa. Detailed P-T estimates must be carried out in order to define this event better. It may represent either subduction-related PT values or a metamorphic imprint within a thickened crust.

Within the GFM, D1 is attributed to T ≤ 420°C and P = 0.45-0.6 GPa (table 1, [29]) and D2 to T = 450-550°C and P = 0.5-0.65 GPa: they are currently interpreted as Variscan orogenic events. D1, D2 and $D1_p$ do not necessarily represent contemporaneous events ; we simply argue that GFM and AFP probably lay at different crustal levels within the Variscan chain (420-350 Ma ; stage A in figure 10).

As stated above, the $D2_p$ event in the AFP developed at low pressure in high heat flow conditions. Such conditions are reported both during the early opening of the Tethyan basin [6, 12, 13, and refs. therein] and at the Carboniferous collapse of the Variscan chain (*e.g.* Gardien *et al.* [61] and refs. therein). In our case, the inferred Carboniferous age strongly supports the second hypothesis. At lower crustal levels, migmatisation of the same age in the Ulten zone (a in figure. 1) indicates that this high heat flow may have benefited from magmatic heat convection [53]. During $D3_p$, again with a relatively high T/P ratio, AFP and GFM, representing rock volumes characterised by contrasting thermo-mechanical evolution were coupled. This feature is reminiscent of the Late Variscan collapse recorded in the French Massif Central by the coupling of the Velay and Pilat units [62, 63] and in the Bohemian Massif by the coupling of the Hilinsko and Svratka regions [64] (stage B in figure 10).

The emplacement of the Brixen granodiorite (282 Ma) may be related to lithospheric thinning, probably evolving to Tethian rifting [13] (event C in figure 10). The AFP and GFM are thus involved in the Alpine orogenesis.

7. Conclusions

The data presented here indicate that the Eastern Southalpine Basement shows different structural and metamorphic records. Rock volumes recording differing thermo-mechanical evolution are coupled during the Middle Carboniferous in greenschist-facies conditions. These new structural and metamorphic data complete the outline of the tectonic evolution in the region.

Several stages of the entire Variscan cycle are recorded within a relatively small area. After D1 and $D1_p$, which probably developed within a thickened crust, $D2_p$ and $D3_p$ show polyphase evolution related to the late orogenic collapse.

Aknowledgements

Field work greatly benefit of the excellent, friendly hospitality and cooking at Rifugio Vallaga/Marburger Hutte in the Sarntal Alps. Suggestions and critical readings by G.V. Dal Piaz, G. Gosso, S. Guillot, B. Lombardo, S. Martin, G. Ranalli, M.I. Spalla, P. Tartarotti, J. von Raumer, and an anonymous referee greatly improved the text. The constructive and detailed review given by M.I. Spalla is greatly appreciated.

References

[1] Niggli, E., Zwart, H.J., Metamorphic Map of the Alps, scale 1:1000000. UNESCO Subcommission for the Cartography of the Metamorphic Belts of the World, Sheet 17 of the Metamorphic Map of Europe, Leiden/ Paris, 1973.

[2] Vai, G.B., Cocozza, T., Tentative schematic zonation of the Hercynian chain in Italy, Bull. Soc. Geol. France 8 (1986) 95-114.

[3] Brodie, K.H. and Rutter, E.H., Deep crustal extensional faulting in the Ivrea Zone of Northern Italy, Tectonophysics 140 (1987) 193-212.

[4] Handy, M.R., The structure, age and kinematics of the Pogallo Fault Zone, Southern Alps, northwestern Italy, Eclogae Geol. Helv. 80 (1987) 593-632.

[5] Schmid, S.M., Zingg, S.M., Handy, M., The kinematics of movements along the Insubric line and the emplacement of the Ivrea Zone, Tectonophysics 135 (1987) 47-66.

[6] Diella, V., Spalla, M.I., Tunesi, A., Contrasting thermomechanical evolutions in the Southalpine metamorphic basement of the Orobic Alps (central Alps, Italy), J. Metam. Geol. 10 (1992) 203-219.

[7] Bertotti, G., Siletto, G.B. Spalla, M.I., Deformation and metamorphism associated with crustal rifting: the Permian to Liassic evolution of the Lake Lugano - Lake Como area (Southern Alps), Tectonophysics 226 (1993) 271-284.

[8] Siletto, G.B., Spalla, M.I., Tunesi, A., Lardeaux, J.M., Colombo, A., Pre-Alpine structural and metamorphic histories in the Orobic Alps, Italy, in: von Raumer, J and Neubauer, F. (Eds.), Pre-Mesozoic Geology in the Alps Springer, Berlin Heidelberg New York, 1993, pp. 585-598.

[10] Spalla, M.I., Gosso, G., Pre-Alpine tectonometamorphic units in the central Southern Alps: structural and metamorphic memory, Mem. Sci. Geol. 51 (1999) 221-229.

[11] Di Paola, S., Spalla, M.I., Contrasting tectonic records in pre-Alpine metabasites of the Southern Alps (Lake Como, Italy), J Geodyn. 30 (2000) 167-189.

[12] Lardeaux, J.M., Spalla, M.I., From granulites to eclogites in the Sesia zone (Italian western Alps): a record of the opening and closure of the Piedmont Ocean, J. metam. Geol. 9 (1991) 35-59.

[13] Dal Piaz, G.V., Evolution of Austro-Alpine and Upper Pennidic basement in the Northwestern Alps from Variscan convergence to post-Variscan extension. in: von Raumer, J and Neubauer, F. (Eds.), Pre-Mesozoic Geology in the Alps Springer, Berlin Heidelberg New York, 1993, pp. 327-344.

[14] Benciolini, L., Metamorphic evolution of the Silvretta gabbro and related rocks (Upper Austroalpine, Central Alps). Its bearing on the pre-Mesozoic history of the Alpine area basement, Mem. Sci. Geol. 46 (1994) 353-371.

[15] Schuster, R., Scharbert, S., Abart, R., Permo-Triassic high temperature/ low pressure metamorphism in Austroalpine basement units (Eastern Alps), Mitt. Österr. Min. Ges. 143 (1998) 383-386.

[16] Colombo, A., Tunesi, A., Pre-Alpine metamorphism of the Southern Alps west of the Giudicarie Line. Schweiz. Mineral, Petrogr. Mitt. 79 (1999) 63-77

[17] Frey, M., Desmons, J., Neubauer, F. (Eds.), The new metamorphic map of the Alps, Schweiz. Mineral. Petrogr. Mitt. 79 (1999) 1-230.

[18] Spalla, M.I., Siletto, G.B., Di Paola, S., Gosso, G., The role of structural and metamorphic memory in the distinction of tectono-metamorphic units: the basement of the Como lake in the Southern Alps, J. Geodyn. 30 (2000) 191-204.

[19] Schuster, R., Proyer, A., Hoinkes, G., Schulz, B., Indications for a Permo-Triassic metamorphic imprint in the Austroalpine crystalline rocks of the Deffereggen Alps (Eastern Tyrol), Mitt. Österr. Min. Ges. 147 (2001) 275-277.

[20] Zanferrari, A., Poli, M.E., Il basamento sudalpino orientale: stratigrafia, tettonica varisica e alpina, rapporti copertura- basamento, Studi Geologici Camerti 2 (1992) 299-302.

[21] Sassi, F.P., Arkai, P., Lantai C., Venturini, C., Location of the boundary between the metamorphic Southalpine basement and the Palaeozoic sequences of the Carnic Alps: illite «crystallinity» and vitrinite reflectance data. Schweiz, Mineral. Petrogr. Mitt. 75 (1995) 399-412.

[22] Poli, M.E., Visona', D., Zanferrari, A., Il basamento varisico delle Dolomiti. 78ª Riunione estiva Soc. Geol. It., S. Cassiano (BZ), 16-18 settembre 1996, Riassunti, p. 4.

[23] Visonà, D., Zanferrari, A., Some constraints on geochemical features in the Triassic mantle of the easternmost Austroalpine-Southalpine domain: evidence from the Karawanken pluton (Carinthia, Austria). Int. J. Earth Sci. 89 (2000) 40-51.

[24] Kalvacheva, R., Sassi, F.P., Zanferrari, A., Acritarch evidence for the Cambrian age of phyllites in the Agordo area (South-Alpine basement of Eastern Alps, Italy), Rev. Palaeobot. Palynol. 48 (1986) 311-326.

[25] Meli, S., Klötzli, U.S., Evidence for Lower Paleozoic magmatism in the Eastern Southalpine basement: zircon geochronology from Comelico porphyroids, Schweiz. Mineral. Petrogr. Mitt. 81 (2001) 147-157.

[26] Poli, M.E., Zanferrari, A., The Agordo basement (NE Italy): a 500 Ma-long geological record in the Southalpine crust, IGCP No. 276, Newsletter 5 (1992) 283-296.

[27] Hammerschmidt, K., Stöckhert, B., A K-Ar and 40Ar/39Ar study on white micas from the Brixen Quartzophyllite, southern Alps. Evidence for argon loss at low temperatures, Contrib. Mineral. Petrol, 95 (1987) 393-406.

[28] Ring, U., Richter, C., The Variscan structural and metamorphic evolution of the eastern Southalpine basement, J. Geol. Soc. London 151 (1994) 755-766.

[29] Cardin, A., Pisani, F., Sassi, P.F., Visonà, D., Zirpoli, G., Le metapeliti e le anfiboliti del basamento sudalpino delle Alpi Sarentine (Alpi orientali), Mem. Sci. Geol. 37 (1985) 379-406.

[30] Mazzoli, C., Sassi, R., Caratteri del metamorfismo ercinico nella fillade sudalpina ad ovest di Bressanone, Mem. Sci. Geol. 40 (1988) 295-314.

[31] Poli, M.E., Zanferrari, A., Eventi plicativi nel cristallino di Agordo (basamento sudalpino orientale), Atti Ticinensi di Scienze della Terra 34 (1991a) 133-144.

[32] Del Moro, A., Sassi, F.P., Zirpoli, G., Preliminary results on the radiometric age of the Hercynian metamorphism in the South-Alpine basement of the Eastern Alps, N. Jahrb. Geol. Paläontol. 12 (1980) 707-718.

[33] Cavazzini, G.C., Del Moro, A., Sassi, F.P., Zirpoli, G., New data on the radiometric age of the Southalpine basement of the Eastern Alps, in: Geologia del Basamento Italiano. Conv in mem. di T. Cocozza, Siena, 21-22 marzo 1991. Abstract volume, p. 30.

[34] Meli S., Klotzli U., Preliminary geochronological results on the pre-Variscan metavolcanics of the eastern southalpine basement. Plinius 18 (1997) 144-145.

[35] Del Moro, A., Visonà, D., The epiplutonic Hercynian Complex of Brixen (Bressanone, Eastern Alps, Italy). Petrologic and radiometric data, N. Jahrb. Mineral. Abh., 145 (1982) 66-85.

[36] Visonà, D., Contributo alla conoscenza del Massiccio di Bressanone, Rend. Soc. It. Min. Petrol. 33 (1977) 647-665.

[37] Visonà, D., Polybaric evolution of calc-alkaline magmas: the dioritic belt of the Bressanone-Chiusa igneous complex (NE Italy), Mem. Sci. Geol. 47 (1995) 11-124.

[38] Morgante, S., Il massiccio granitico di Bressanone (Alto Adige), Mem. Museo Tridentino Sci. Nat. 20 (1974) 67-157.

[39] D'Amico, C., Del Moro, A., Permian and Triassic Rb-Sr dating in the Permian rhyodacitic ignimbrites of Trentino (Southern Alps), Rend. Soc. It. Mineral. Petrol. 43 (1988) 171-180.

[40] Sander, B., Carta geologica delle Tre Venezie 1:100.000. Foglio Bressanone, Sez. geol. Uff. Idrogr. Mag. alle Acque, Venezia, 1924.

[41] Scolari, A., Zirpoli, G., Fenomeni di metamorfismo di contatto nella fillade sudalpina indotti dal massiccio granitico di Bressanone (Alto Adige), Mem. Museo Trid. Sci. Nat. 18 (1971) 173-222.

[42] Sassi, F.P., Spiess, R., The South-Alpine Metamorphic Basement in the Eastern Alps, in: von Raumer, J and Neubauer, F. (Eds.), Pre-Mesozoic Geology in the Alps Springer, Berlin Heidelberg New York, 1993, pp. 599-607.

[43] Sassi, F.P., Neubauer, F., Mazzoli, C., Sassi, R., Spiess, R., Zirpoli, G., A tentative comparison of the Palaeozoic evolution of the Austroalpine and Southalpine Quartzphyllites in the Eastern Alps, Per. Mineral. 63 (1994) 35-52.

[44] Castiglioni, G.B., The Quaternary of the Bressanone basin, revisited, Geol. Insubr. 2 (1997) 121-127.

[45] Bell, T.H., Rubenach, M.J., Fleming, P.D., Porphyroblast nucleation, growth and dissolution in regional metamorphic rocks as a function of deformation partitioning during foliation development, J. Metam. Geol. 4 (1986) 37-67.

[46] Vernon, R.H., Growth and concentration of fibrous sillimanite related to heterogeneous deformation in K-feldspar-sillimanite metapelites, J. Metam. Geol. 5 (1987) 51-68.

[47] Xu, G., Will, T.M., Powell, R., A calculated petrogenetic grid for the system K2O-FeO-MgO-Al2O3-SiO2-H2O, with particular reference to contact-metamorphosed pelites, J. Metam. Geol. 12 (1994) 99-119.

[48] Castro, A., On granitoid emplacement and related structures. A review, Geol. Rundsch. 76 (1987) 101-124.

[49] Paterson, S. R., Vernon, R. H., Fowler, T.K. Jr., Aureole tectonics, in: Kerrick, D.M. (Ed.), Contact metamorphism, Review in Mineralogy Volume 26, Mineralogical Society of America, 1991, pp. 673-722.

[50] Bakos, F., Del Moro, A., Visonà, D., The Hercynian volcano-plutonic association of Ganna (Lake Lugano, Central Southern Alps, Italy), Eur. J. Mineral. 2 (1990) 373-383.

[51] Barton, M.D., Staude, J-M., Snow, E.A. and Johnson, D.A., Aureole systematics, in: Kerrick, D.M. (Ed.), Contact metamorphism, Review in Mineralogy Volume 26, Mineralogical Society of America, 1991, pp. 723-747.

[52] Neubauer, F., The Variscan orogeny in the Austroalpine and Southalpine domains of the Eastern Alps, Schweiz. Min. Petr. Mitt. 68 (1988) 339-349.

[53] Godard, G., Martin, S., Prosser, G., Kienast, J.R., Morten, L., Variscan migmatites, eclogites and garnet peridotites of the Ulten zone, Eastern Austroalpine system, Tectonophysics 259 (1996) 313-341.

[54] Poli, M.E., Zanferrari, A., La zona di taglio duttile della seconda fase ercinica nel cristallino di Agordo (basamento sudalpino orientale), Atti Ticinensi di Scienze della Terra 34 (1991b) 167-174.

[55] Sassi, F.P., Il cristallino sudalpino di Bressanone. in: AAVV Note illustrative del F° Brennero della Carta geologica d'Italia, Padova, 1968, pp 1-10.

[56] Sassi, F.P., Zanferrari, A., Zirpoli, G., Some considerations on the South-Alpine basement of the Eastern Alps, N. Jahrb. Geol. Paläont. Mh. 10, (1974) 609-624.

[57] Passchier, C.W., Myers, J.S., Kröner, A., Field geology of high grade gneiss terrains. Springer Verlag, Berlin, 1990, 150 p.

[58] Williams, P., 1985. Multiply deformed terrains - problems of correlations. J. Struct. Geol. 7, 269-280.

[59] Spalla, M.I., Gosso, G., Siletto, G.B., Di Paola, S., Magistroni C., Strumenti per individuare unità tettono-metmorfiche nel rilevamento geologico del basamento cristallino, Mem. Sci. Geol. 50 (1998) 155-164.

[60] Spalla, M.I., Zucali, M., Di Paola, S., Gosso, G., A critical assessment of the tectono-thermal memory of rocks and definition of tectono-metamorphic units: evidence from fabric and degree of metamorphic transformations. in: Gaspais, D., Brun, J.P., Cobbold, P.R. (Eds.), Deformation Mechanisms, Rheology and Tectonics: from Minerals to the Lithosphere, Geological Society, London, Special Publications 243, 2005, 227-247.

[61] Gardien, V., Lardeaux, J.M., Ledru, P., Allemand, P., Guillot, S., Metamorphism during late orogenic extension. Insights from the French Variscan Belt, Bull. Soc. Géol. France 168 (1997) 271-286.

[62] Gardien, V., Tegey, M., Lardeaux, J.M., Misseri, M., Dufour, E., Crust-mantle relationships in the French Variscan Chain: the example of the Southern Monts du Lyonnais unit (eastern French Massif Central), J. Metam. Geol. 8 (1990) 477-492.

[63] Montel, J.M., Marignac, C., Barbey, P., Pichavant, M., Thermobarometry and granite genesis: the Hercynian low-P, high-T Velay anatectic dome (French Massif Central), J. Metam. Geol. 10 (1992) 1-15.

[64] Pitra, P., Guiraud, M., Probable anticlockwise P-T evolution in extending crust: Hlinsko region, Bohemian Massif, J. Metam. Geol. 14 (1996) 49-60.

[65] Plyusnina, L.P., Geothermometry and geobarometry of plagioclase-hornblende bearing assemblages, Contrib. Mineral. Petrol. 80 (1982) 140-146.

[66] Ghent, E.D., Stout, M.Z., Geobarometry and geothermometry of plagioclase – biotite – garnet – muscovite assemblages, Contrib. Mineral. Petrol. 76 (1981) 92-97.

[67] Massonne, H.J., Schreyer, W., Phengite geobarometry based on limiting assemblage with K-feldspar, phlogopite and quartz, Contrib. Mineral. Petrol. 96 (1987) 212-224.

[68] Ganguly, J., Saxena, S.K., Mixing properties of alumino silicate garnets: constraints from natural and experimental data and application to geothermobarometry, Am. Mineral. 69 (1984) 88-97.

[69] Hoinkes, G., Effect of grossular-content in garnet on partitioning of Fe and Mg between garnet and biotite, Contrib. Mineral. Petrol. 92 (1986) 393-399.

[70] Guidotti, C.V., Sassi, F.P., Classification and correlation of metamorphic facies series by means of muscovite b_0 data from low-grade metapelites, N. Jahrb. Mineral. 153 (1985) 363-380.